1 Motivation: Towards a complete census of low-mass AGNs

As a means of constraining different primordial black hole (BH) seeding scenarios (e.g., Volonteri 2010; Bellovary et al. 2011; Greene 2012; Reines & Comastri 2016), much effort has been made in searches for active galactic nuclei (AGNs) powered by intermediate-mass black holes (IMBHs, $10^4 M_\odot \leq M_{\rm BH} \leq 10^6 M_\odot$) in the centers of local low-luminosity galaxies. To date, the largest samples of low-mass AGNs[1] come from studies that search for AGN signatures in low-redshift ($z \lesssim 0.3$), low-luminosity galaxies in large optical spectroscopic surveys such as SDSS (e.g., Greene & Ho 2007; Barth et al. 2008; Reines et al. 2013; Moran et al. 2014). While these studies have provided crucial first steps toward understanding the IMBH-powered low-mass AGN population, **obscured low-mass AGNs are still missing in current studies**. This is primarily due to optical low-mass AGNs being either selected based on the presence of broad emission lines (i.e., unobscured) or lacking the crucial X-ray observations to confirm the presence of obscuring material.[2] On the other hand, studies with infrared spectroscopy and/or X-ray observations have consistently shown that more than 50% of the AGNs with luminosities comparable to those of IMBH-powered AGNs are actually obscured (e.g., Goulding et al. 2010, 2011, Ricci et al. 2016). **Therefore, many or even most of the accreting IMBHs remain elusive.**

Recently, we have shown that obscured low-mass AGNs can be identified by combining optical spectroscopic, mid-IR, and X-ray observations (Chen et al. 2017a). Due to the limited area of current deep extragalactic X-ray surveys, only an extremely small number of low-mass AGNs are found to be X-ray obscured (i.e., $N_{\rm H} \gtrsim 10^{22}$ cm^{-2}), including one AGN discovered in the *NuSTAR* serendipitous survey (Chen et al. 2017a), and an optically selected Seyfert 2 galaxy with *XMM-Newton* follow-up observations (Thornton et al. 2009). Collecting a larger sample of X-ray obscured low-mass AGNs in the local universe is, therefore, essential for using IMBHs reliably as a boundary condition to study different BH-seed formation and galaxy evolution scenarios.

Search for obscured low-mass AGNs with X-rays and optical emission lines: The key to revealing the obscured low-mass AGN population is high spatial resolution X-ray observations because these can effectively avoid confusion due to diffuse X-ray emission and off-nuclear ultra-luminous X-ray sources (ULXs) while confirming the presence of intervening gas/dust toward the AGN. Currently, there are only ~ 10 low-mass Seyfert 2 galaxies with follow-up observations in X-rays.[3] Intriguingly, all of them have X-ray fluxes 10 to > 100 times lower than the expected values based on the tight $L_{\rm X} - L_{\rm [OIII]}$ relation for typical AGNs (Figure 1–left). Low-mass AGNs with similarly weak X-ray emission (compared to [O III], UV continuum, or broad emission lines) were also found in several type 1 systems with *XMM-Newton* or *Chandra* observations (e.g., Dong et al. 2012, Plotkin et al. 2016, Simmonds et al. 2016, Baldassare et al. 2017; also see Figure 1–left). Many of these previous observations have very limited X-ray counts that prohibit even basic hardness-ratio spectral shape analysis. The lack of X-ray emission in these sources remains an open question (e.g., Plotkin et al. 2016, Baldassare et al. 2017).

A *Spitzer*/IRS sample of Seyfert 2 low-mass AGNs: At higher redshift ($z \sim 1$), X-ray stacking analyses have suggested that star-forming dwarf galaxies host a substantial population of obscured AGNs (Xue et al. 2012, Mezcua et al. 2015). It is therefore *unlikely* that the majority

---

[1]We refer to AGNs hosted by low-mass galaxies with $M_\star < 10^{10} M_\odot$ as "low-mass" AGNs. They are usually powered by accretion onto IMBHs (e.g., Reines et al. 2013).

[2]For low-luminosity Seyfert 2 galaxies, the lack of broad emission lines alone is not conclusive evidence for the presence of obscuration; see Trump et al. (2011) and Elitzur et al. (2014) for details.

[3]*Chandra* ObsID 13969–13974 (Moran 2011), XMM ObsID 0740620301 (Schawinski 2014), Thornton et al. (2009), Chen et al. (2017).
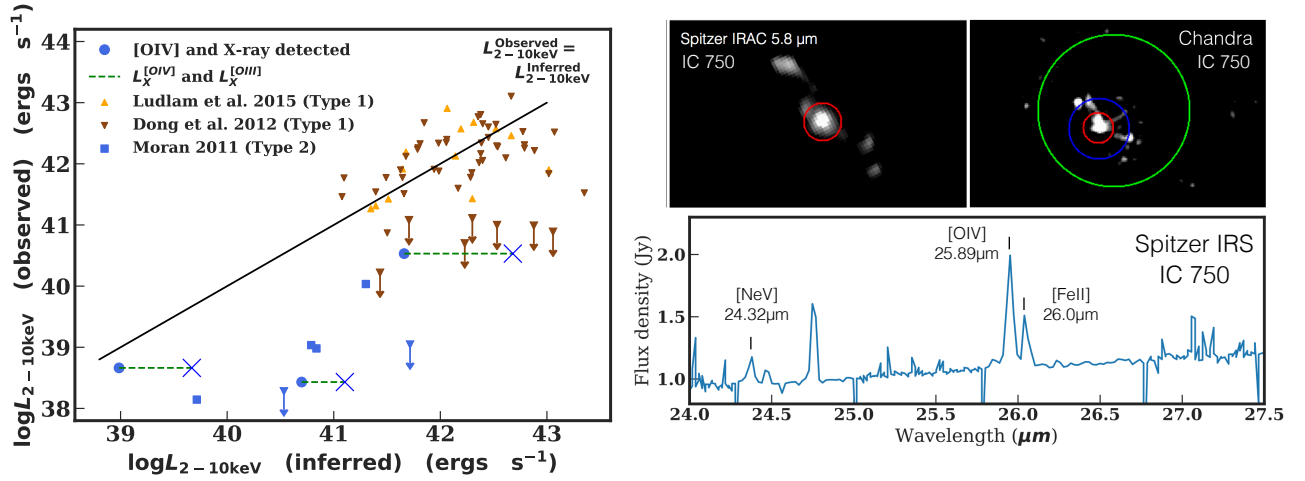
Figure 1 – *Left:* L_X^{Observed} vs. L_X^{Inferred} based on the Panessa et al. (2006) $L_X - L_{[\text{OIII}]}$ relation. Many Seyfert 1 galaxies have $L_X^{\text{Observed}} \sim L_X^{[\text{OIII}]}$, but the majority of Seyfert 2 galaxies have very weak L_X^{Observed} compared to $L_X^{[\text{OIII}]}$. This may simply be caused by host-galaxy contamination of their $L_{[\text{OIII}]}$. On the other hand, the $L_X^{[\text{OIV}]}$ for three low-mass AGNs with IRS spectra (blue circles, derived based on the Goulding et al. 2010 $L_X - L_{[\text{OIV}]}$ relation) suffers from less host-galaxy contamination than their $L_X^{[\text{OIII}]}$ (blue crosses). However, the existing sample with both [O IV] and X-ray observations is extremely small, and only two of them are Seyfert 2 galaxies. *Right:* Illustration of the synergy between *Chandra* and *Spitzer* for IC 750 (Chen et al. 2017 and *Spitzer* archival data). The green ($25''$ radius), blue ($10''$ radius), and red ($5''$ radius) circles represent the *NuSTAR*, *Chandra*, and optical locations, respectively. For this source, the [O IV] and [Ne V] lines from *Spitzer* IRS provide the unobscured accretion-rate indicator, and only *Chandra* has the requisite spatial resolution for separating off-nuclear X-ray sources from the AGN for studying the properties of nuclear obscuration.

of the local low-mass AGNs are either unobscured or intrinsically X-ray weak. The *relatively* weak X-ray emission might simply be caused by the fact that optical emission lines are *not* robust tracers of IMBH accretion rates for low-luminosity obscured AGNs, since they are either susceptible to the presence of intervening dust (e.g., Hα and He II 4685 Å) or suffer from severe host-galaxy contamination (e.g., [O III] 5007 Å, see Trump et al. 2015). **For obscured low-mass AGNs, the expected X-ray fluxes derived based on optical emission lines are not reliable**. On the other hand, mid-IR fine-structure lines such as [O IV] $25.89\mu m$ and [Ne V] $14.32, 24.32\mu m$ require an ionizing continuum harder than those of typical optical emission lines and are not sensitive to intervening dust (Meléndez et al. 2008). Mid-IR observations can also trace emission from star-forming gas/dust (e.g., the PAH features) that can be used to better isolate AGN emission, but they cannot provide evidence of the presence of absorbing gas. Therefore, the synergy between *Spitzer* IRS and sensitive, high-resolution X-ray observations from *Chandra* might be the only means for systematically revealing the obscured AGN population powered by IMBHs. To date, only two low-mass Seyfert 2s with detections of mid-IR high-ionization lines have been observed by X-ray facilities, and their X-ray properties suggest that they are indeed X-ray obscured AGNs (see Sec. 2 where the properties of the two objects will be fully presented).[4] We propose to obtain *Chandra* observations of four low-luminosity Seyfert 2 galaxies hosting IMBH candidates with mid-IR emission-line detections. This will triple the sample size of such systems with both IRS and X-ray measurements, and **establish the first statistically significant sample of obscured low-mass AGNs**.

2 Hunting for obscured low-mass AGNs with *Chandra* and *Spitzer*

Sample Selection: The proposed four obscured low-mass AGNs are culled from the low-velocity-dispersion Seyfert 2 galaxy sample selected from the SDSS by Barth et al. (2008). Recently, Hood et al. (2017) have studied the *Spitzer* IRS spectra for a subset of 19 galaxies from the Barth et al.

---

[4] J1109 (Thornton et al. 2009) and IC 750 (Chen et al. 2017)

(2008) sample. The [O IV] $25.89\mu m$ emission line is robustly detected in eight of the 19 galaxies. The [O IV] $25.89\mu m$ line has a much higher ionization energy than those of [OIII] 5007 Å (e.g., Meléndez et al. 2008), making it much less affected by host-galaxy contamination. We select the four galaxies with the highest [O IV] $25.89\mu m$ line fluxes for this proposal. Based on their low velocity dispersion ($\sigma_{\rm Bulge}$) and the well-established $M_{\rm BH} - \sigma_{\rm Bulge}$ relation in the local universe (e.g., Tremaine et al., 2002), they are likely powered by accretion onto IMBHs.

Simulated spectra and count rate estimations: All of our proposed targets have a mid-IR spectral index ($\alpha_{20-30\mu m}$) less than -1, suggesting small starburst contributions at mid-IR wavelengths (e.g., Deo et al. 2009). Their PAH-inferred star formation rates also indicate that their $L_{\rm [OIV]}$ have negligible host-galaxy contamination. Therefore, we can reliably estimate the expected $L_{\rm X}$ using the well-established $L_{\rm [OIV]} - L_{\rm X}$ relations (e.g., Meléndez et al. 2008; Goulding et al. 2010; LaMassa et al. 2010). We make use of the [O IV] luminosities calculated based on the *Spitzer* IRS observations (Hood et al. 2017), and the $L_{2-10\rm keV}^{\rm intrinsic} - L_{\rm [OIV]}$ relation reported in Goulding et al. (2010)[5] to estimate the expected intrinsic X-ray fluxes. To ensure the proposed observations will yield robust detections, we conservatively assumed all of our targets have intrinsic $L_{2-10\rm keV}$ values 1σ lower (by ~ 0.15 dex for the luminosity range of our sample[6]) than the Goulding et al. (2010) relation and are heavily obscured ($N_{\rm H} = 10^{23}$ cm^{-2}) in addition to Galactic absorption. Assuming a simple power-law spectrum with $\Gamma = 1.8$, we created simulated spectra using XSPEC and the response matrix and ancillary file suitable for Cycle 20. The estimated count rates for this very conservative assumption, along with the basic properties of our sample, are shown in Table 1. We also fit the simulated spectra with the Cash statistic with the same model where Γ is fixed at 1.8, and $N_{\rm H}$ is free to vary. We create 100 simulated spectra, and found that the average 90% confidence interval is $N_{\rm H} = (0.7 - 1.6) \times 10^{23}$ cm^{-2} for spectra with ≈ 10 counts. We reiterate that this is a conservative estimation, and the uncertainties would already be sufficiently small to constrain the obscuration properties of low-mass galaxies thanks to the high spatial resolution and low background of *Chandra*. In reality, we expect our sample to have $N_{\rm H}$ distribution and $L_{2-10\rm keV}^{\rm intrinsic} - L_{\rm [OIV]}$ similar of those of typical Seyfert galaxies (e.g., Merloni et al. 2013, Goulding et al. 2010). Therefore, we also list the expected count rates derived for the same sources assuming $N_{\rm H} = 10^{22}$ cm^{-2} in Table 1.

Feasibility based on existing data: We further assess the feasibility using the two X-ray obscured low-mass Seyfert 2 galaxies with [O IV] detections. First is J1109 (Thornton et al. 2009). Based on its $L_{\rm [OIV]} - L_{2-10\rm keV}$ ratio, this object is expected to be moderately X-ray obscured, which is supported by its *XMM-Newton* hardness ratio. Due to the limited spatial resolution and higher background level of *XMM-Newton*, and potential host galaxy contaminations, its column density cannot be spectroscopically confirmed. This highlights the importance of using a reliable AGN accretion rate tracer and the high spatial resolution *Chandra* observations. Second is IC 750, a dwarf galaxy and a Compton-thick AGN candidate (Chen et al. 2017a). The *Chandra* observation reveals that an X-ray point source (with angular size less than $2''$) is indeed located at the optical centroid of the galaxy (Figure 1–right), but its observed soft X-ray luminosity ($L_{2-10\rm keV}$) is only 2.7×10^{38} erg s^{-1}. The luminous [O IV] and [Ne V] emission lines and the relatively weak star formation lines provide strong evidence supporting the presence of an AGN in IC 750, demonstrating that the synergy of *Spitzer* and *Chandra* can reveal the presence of heavily obscured AGN in low-mass galaxies. Notably, the large difference between $L_{2-10\rm keV}$ and $L_{2-10\rm keV}^{\rm [OIV]}$ suggests the presence of Compton-thick obscuring material, which is supported by the *NuSTAR* detection of this

---

[5]Goulding et al. (2010) derived the relation by first converting $L_{2-10\rm keV}$ to the bolometric luminosity assuming the Marconi et al. (2004) bolometric correction factors. We have taken this into account when deriving the expected $L_{2-10\rm keV}^{\rm intrinsic}$ from $L_{\rm [OIV]}$.

[6]Based on the Eq. 4 of Goulding et al. 2010.

Table 1. Properties of the obscured low-mass AGN targets

Name	Redshift	g mag	$M_{\rm BH}$ (log $M_\odot$)	$L_{\rm [OIV]}$ (log ergs s^{-1})	0.5–2 keV[a] cts ks^{-1}	2–7 keV[a] cts ks^{-1}	*Chandra* Exp (ks)
J021405.9−001637.0	0.0374	17.4	5.8	39.2	1.3 (< 0.01)	1.9 (0.6)	17
J091414.3+023801.8	0.0735	18.2	5.9	39.9	1.6 (< 0.01)	2.0 (0.8)	15
J094716.1+534944.9	0.0382	17.7	5.6	39.2	1.3 (< 0.01)	1.8 (0.6)	17
J162917.4+425439.8	0.0354	17.9	5.8	39.4	2.2 (0.01)	3.2 (1.0)	10

Note. — Basic properties of our proposed targets. $M_{\rm BH}$ is estimated based on the velocity dispersion measured by Barth et al. (2008) and the Tremaine et al. (2002) $M_{\rm BH} - \sigma$ relation. [a] : The expected *Chandra* count rates in the 0.5–2 and 2–7 keV bands. These values were estimated based on $L_{\rm [OIV]}$ and the Goulding et al. (2010) $L_{\rm [OIV]}$-$L_{\rm 2-10keV}$ relation, assuming a $\Gamma = 1.8$ power-law spectrum and $N_{\rm H} = 10^{22}$ cm^{-2} column density. The conservative values in parentheses are estimated based on a similar spectrum assuming all of the sources have $L_{\rm 2-10keV}$ values that are 1σ lower than the Goulding et al. (2010) relation with $N_{\rm H} = 10^{23}$ cm^{-2}.

source (Chen et al. 2017a), but *NuSTAR* does not have sufficient sensitivity and spatial resolution at < 10 keV for confirming the location of this object and for isolating the AGN from the diffuse thermal emission. *Chandra* observations are essential for identifying low-mass Compton-thick AGN candidates such as IC 750. Neither of the two X-ray obscured low-mass AGNs discussed here are found to be "intrinsically X-ray weak" as suggested by the large difference between their $L_{\rm X}$ and [O III] luminosity shown in Figure 1-left, suggesting that our IRS-characterized sources are indeed an ideal sample for studying obscured low-mass AGNs when combined with the critically required *Chandra* observations.

3 Revealing the X-ray obscured IMBH AGNs

ACIS onboard *Chandra* will efficiently survey the proposed four targets with a total of 57 ks exposure time (Table 1), and will enable the basic X-ray spectral analysis for confirming the obscuring column density for moderately obscured sources with > 10 counts in the 0.5–7 keV band. Given the strong [O IV] emission and considering the $N_{\rm H}$ distribution for typical Seyfert 2 galaxies (e.g. Merloni et al. 2013), we expect that most of the proposed sources will be detected by *Chandra* with more than 10 counts (see Sec. 2). For the unlikely case in which more than one source has little to no photons detected in the *Chandra* hard-band, we will employ X-ray stacking techniques to put a constraint on the average spectral shape for such sources and determine possible future *NuSTAR* observations to study the Compton-thick ($N_{\rm H} > 1.5 \times 10^{24}$ cm^{-2}) candidates that can be identified with the proposed *Chandra* observations. With the synergy between high-ionization mid-IR lines identified using *Spitzer* IRS spectra and high spatial resolution *Chandra* images, our proposed sample will enable the first systematic study of obscured low-mass AGNs spanning a wide range of obscuring column densities. This will provide a key step toward understanding the full AGN population powered by IMBHs. **Combining with previous studies of low-mass AGNs, we aim to place constraints on the obscured fraction for low-mass AGNs and provide valuable insights into IMBH accretion physics.**

References: ● Baldassare et al., 2017ApJ...836...20B ● Barth et al., 2008AJ....136.1179B ● Bellovary et al., 2011ApJ...742...13B ● Brandt & Alexander, 2015A&ARv..23....1B ● Chen et al., 2017, 2017ApJ...837...48C ● Darling, 2014cxo..prop.4410D ● Deo et al., 2009ApJ...705...14D ● Dong et al., 2012ApJ...761...73D ● Elitzur et al., 2014MN-RAS.438.3340E ● Goulding et al., 2010MNRAS.406..597G ● Greene & Ho 2007ApJ...670...92G ● Greene 2012NatCo...3E1304G ● Hood et al., 2017, ApJ in press ● LaMassa et al., 2010ApJ...720..786L ● Ludlam et al., 2015MNRAS.447.2112L ● Mezcua et al., 2015arXiv151105844M ● Meléndez et al., 2008ApJ...682...94M ● Merloni et al., 2014MNRAS.437.3550M ● Moran, E., 2011cxo..prop.3434M, 2014AJ....148..136M ● Panessa et al., 2006A&A...455..173P ● Plotkin et al., 2016ApJ...825..139P ● Reines et al., 2013ApJ...775..116R ● Reines & Comastri, 2016arXiv160903562R ● Simmonds et al., 2016AA...596A..64S ● Thornton et al., 2009ApJ...705.1196T ● Tremaine et al., 2002ApJ...574..740T ● Trump et al., 2011ApJ...733...60T, 2015ApJ...811...26T ● Volonteri 2010A&ARv..18..279V ● Xue et al., 2012ApJ...758..129X